Letters

Analytically Assessing the Effect of Strength on Temporary Overvoltage in Hybrid Multi-Infeed HVdc Systems

Hao Xiao, *Member, IEEE*, Xianzhong Duan, *Senior Member, IEEE*, Yi Zhang, *Fellow, IEEE*, and Yinhong Li, *Senior Member, IEEE*

***Abstract*—In hybrid multi-infeed HVdc (HMIDC) systems comprising both voltage-source and line-commutated converters' inverters, the strength has a significant effect on the temporary overvoltage (TOV). However, this effect has always been assessed by the simulated approach in earlier works. It is unable to provide the sufficiently theoretical perspectives and also time-consuming as onerous electromagnetic transient simulations are required. Therefore, in this letter, the mathematical expression of the TOV is first derived as the analytical function of the hybrid multi-infeed interactive effective short-circuit ratio (HMIESCR) strength index. This derivation is achieved by using the quasi-steady-state analytical model of HMIDC systems with the interinverter interactions considered. Then, the derived expression is utilized for analytically assessing the effect of the HMIESCR on the TOV versus various system parameters and operation variables. Compared to the simulated approach, the proposed analytical approach here can offer more sufficiently theoretical perspectives and is also more efficient as simulations are no more required. Finally, the experimental results of a hybrid tri-infeed HVdc test system based on the hardware-in-the-loop platform validate the analytical approach.**

***Index Terms*—Hybrid multi-infeed HVdc (HMIDC) systems, hybrid multi-infeed interactive effective short-circuit ratio (HMIESCR), interinverter interactions, strength, temporary overvoltage (TOV).**

I. Introduction

RECENTLY, hybrid multi-infeed HVdc (HMIDC) systems have been increasingly arising where both voltage-source and line-commutated converters (VSC and LCC) are located at various inverter ac buses in the common receiving end ac network [1]–[3]. One typical example of such systems is China Guangdong Power Grid in 2021 including one newly commissioned VSC and nine LCC inverters [4], [5]. In HMIDC systems, the blocking of the LCC inverter due to disturbances such as ac and dc faults may cause the temporary overvoltage (TOV) at the concerned inverter ac bus. The higher TOV will impose a great threat to the electrical equipment security in the LCC inverter such as thyristor valves, converter transformers, and reactive power compensators [6], [7]. Besides, the TOV is expected to be significantly affected by the strength since the latter essentially quantifies the voltage support capability of the receiving end ac network to the normal operation of the concerned LCC inverter [6]. Thereby, it is very helpful to assess the effect of the strength on the TOV in HMIDC systems.

The initial research on the effect of the strength on the TOV has been mainly conducted in single-infeed LCC-HVdc systems including only single inverter. Therein, the classical effective short-circuit ratio (ESCR) strength index is identified to affect the TOV inversely in the IEEE Standard 1204-1997 through the parametric analysis [7]. Buoyed by the extensive application of the ESCR in single-infeed LCC-HVdc systems, its further usage for the TOV study in multi-infeed LCC-HVdc systems has been subsequently explored [8]. However, this exploration indicates that the ESCR cannot be effectively utilized for the accurate prediction of the TOV. This is because the interinverter interactions existing among multiple LCC inverters within the common receiving end ac network are not considered in the definition of the ESCR concept. To address such issue, the multi-infeed interaction factor (MIIF) index is therefore developed to quantify the interinverter interactions in multi-infeed LCC-HVdc systems by the CIGRE Working Group B4.41 [6]. The use of the MIIF then enables the multi-infeed interactive ESCR (MIESCR) strength index to be further proposed [6]. Thereafter, the MIESCR is also reported to affect the TOV with an inverse relationship by the simulated analysis [6], [9]. Nevertheless, the above conclusions as to the impact of the strength on the TOV in multi-infeed LCC-HVdc systems cannot be directly extended into the concerned HMIDC systems in this letter. This is caused by the fact that there are more complex interinverter interactions in HMIDC systems since VSC and LCC inverters have obviously different operation principles and consequently various electrical characteristics [5].

Manuscript received July 16, 2021; revised August 20, 2021; accepted September 9, 2021. Date of publication September 14, 2021; date of current version November 30, 2021. This work was supported by the National Natural Science Foundation of China under Grant 51907067. *(Corresponding author: Yinhong Li.)*

Hao Xiao is with the Department of Electrical and Computer Engineering, University of Manitoba, Winnipeg, MB R3T 2N2, Canada. (e-mail: xiaohao_hvdc@163.com).

Xianzhong Duan and Yinhong Li are with the State Key Laboratory of Advanced Electromagnetic Engineering and Technology, Hubei Electric Power Security and High Efficiency Key Laboratory, School of Electrical and Electronic Engineering, Huazhong University of Science and Technology, Wuhan 430074, China. (e-mail: xzduan@hust.edu.cn; liyinhong@hust.edu.cn).

Yi Zhang is with RTDS Technologies, Inc., Winnipeg, MB R3T 2E1, Canada. (e-mail: yzhang@rtds.com).

Color versions of one or more figures in this article are available at https://doi.org/10.1109/TPEL.2021.3112606.

Digital Object Identifier 10.1109/TPEL.2021.3112606

Although some related research efforts have been made to evaluate the impact of the apparent increase in SCR (AISCR) strength index on the TOV in HMIDC systems [10], [11], this evaluation scheme is always achieved by the simulated approach. The simulated approach causes the following two aspects of limitations in earlier works [10], [11].

1) *Lack of the related mathematical model:* The simulated approach is essentially realized using the electromagnetic transient simulations, which however cannot provide the mathematical model related to both the strength and TOV in HMIDC systems. As a result, it is unable to offer the sufficiently theoretical perspectives for understanding the effect of the strength on the TOV either.
2) *Time-consuming evaluation:* The simulated approach inevitably requires onerous electromagnetic transient simulations to be conducted. It is conceivable that these simulations are very time-consuming. Moreover for future large-scale HMIDC systems with more and more VSC and LCC inverters integrated into, the entire simulation time is even unacceptable for the planning and operation departments of the practical power grid.

Facing the above issues, there is thus a strong motivation to analytically assess the effect of the strength on the TOV in HMIDC systems. For this purpose, the following contributions are made by our work in this letter.

1) *Proposing the related mathematical model:* The hybrid MIESCR (HMIESCR) index, developed with the interinverter interactions quantified by the multi-infeed voltage interaction factor (MVIF) index, is first used to depict the strength of HMIDC systems [12], [13]. Also, the mathematical expression of the TOV is derived as the analytical function of the HMIESCR using the system quasi-steady-state model. Compared with the simulated approach [10], [11], the proposed analytical approach here can provide more sufficiently theoretical perspectives.
2) *More efficient assessment:* The above derived mathematical expression is further used for analytically assessing the effect of the HMIESCR on the TOV versus various system parameters and operation variables in HMIDC systems. Compared to the simulated approach, the analytical approach is more efficient because no time-consuming electromagnetic transient simulations are required at all.

The rest of this letter is organized as follows. In Section II, the mathematical expression of the TOV as the analytical function of the HMIESCR is derived. In Section III, the effect of the HMIESCR on the TOV is analytically assessed. Section IV validates the proposed analytical approach by the experimental results. Finally, Section V concludes this letter.

II. Deriving the Mathematical Expression of the TOV as the Analytical Function of the HMIESCR

A. Classical Model of HMIDC Systems for the TOV Analysis

The schematic diagram of the classical model of HMIDC systems with both VSC and LCC inverters located at inverter ac buses 1 to n in the common receiving end ac network is given in Fig. 1 for the TOV analysis. Therein, all ac subsystems 1 to n are represented by their Thevenin impedances and sources. The interinverter interactions are physically reflected by the tie-line impedances among various inverter ac buses. Moreover, the system parameters and operation variables are expressed in pu with visually self-explanatory notations. Also in the subsequent analysis, the rated dc active power of LCC inverter 1 (P_{d1N}) is set as the base MVA power while the rated ac voltage of the common receiving end network (U_N) is deployed as the base voltage.

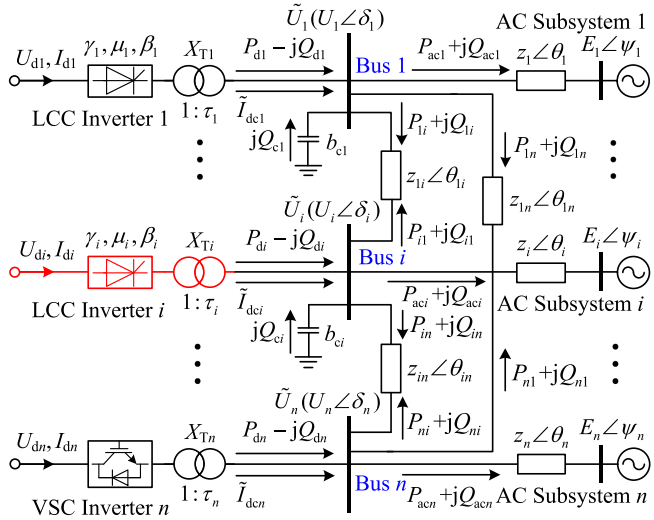

Fig. 1. Schematic diagram of the classical model of HMIDC systems including n VSC and LCC inverters for the TOV analysis.

B. Deriving the Mathematical Expression of the TOV

When LCC inverter i ($i \in \{1, 2, \ldots, n-1, n\}$) in Fig. 1 is blocked due to external disturbances such as ac and dc faults, the reactive power consumption Q_{di} is accordingly absent. However, the compensators of shunt filters and capacitor banks attached at LCC inverter ac bus i are still in service. This means that the excessive reactive power supplied by the compensators (Q_{ci}) is flowing into the common receiving end ac network instead. Consequently, the TOV arises at various inverter ac buses with the highest level presented at LCC inverter ac bus i.

To calculate the TOV at LCC inverter ac bus i (hereafter called TOV$_i$), the equivalent single-infeed LCC-HVdc model of HMIDC systems in Fig. 1 is further developed in Fig. 2 [13]. Therein, $\tilde{Y}_{\mathrm{eq}i}$(the tilde denotes the complex electrical quantity in this letter) is the equivalent admittance of HMIDC systems referred at LCC inverter ac bus i and is equal to ($\tilde{Y}_{ii}+\tilde{Y}_{\mathrm{vir}i}$) [13]. Note that$\tilde{Y}_{ii}$ is the nodal self-admittance matrix element at LCC inverter ac bus i, and $\tilde{Y}_{\mathrm{vir}i}$ is called the virtual admittance indicative of the aggregate impact of all other inverters on the concerned LCC inverter i. Furthermore, $\tilde{Y}_{\mathrm{vir}i}$ is expressed as

$$\tilde{Y}_{\mathrm{vir}i} = \sum_{j\neq i, j=1}^{n} \tilde{Y}_{ij} \cdot \mathrm{MVIF}_{ji} \tag{1}$$

$$\begin{aligned}\mathrm{TOV}_i &= \sqrt{U_i^2 + \frac{P_{di}^2+Q_{di}^2}{U_i^2 Y_{eqi}^2} + \frac{2Q_{di}}{Y_{eqi}}} \\ &= \sqrt{U_i^2 + \frac{P_{di}^2+Q_{di}^2}{U_i^2 P_{di}^2 \cdot \mathrm{HMIESCR}_i^2/U_i^4} + \frac{2Q_{di}}{P_{di}\cdot \mathrm{HMIESCR}_i/U_i^2}} \\ &= U_i\sqrt{1+\frac{2Q_{di}}{P_{di}}\cdot\frac{1}{\mathrm{HMIESCR}_i} + \frac{P_{di}^2+Q_{di}^2}{P_{di}^2}\cdot\frac{1}{\mathrm{HMIESCR}_i^2}}.\end{aligned}$$

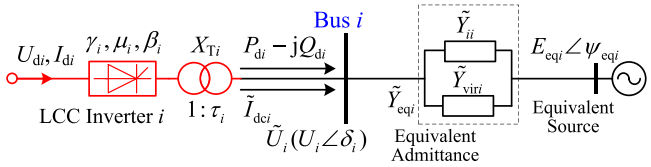

Fig. 2. Equivalent single-infeed LCC-HVdc model of HMIDC systems referred at LCC inverter ac bus i.

where $\tilde{Y}_{ij}$ represents the nodal mutual-admittance matrix element between inverter ac buses j ($j\in\{1, 2, \ldots, n-1, n\}$, $j \neq i$) and i. Meanwhile, MVIF_{ji} is defined as the ratio of the magnitudes of the voltage vector changes at inverter ac buses j and i in Fig. 1(i.e., $|\Delta\tilde{U}_j|/|\Delta\tilde{U}_i|$) and utilized for quantifying the interactions between inverters j and i in HMIDC systems [12]. Note also that $E_{eqi}\angle\psi_{eqi}$ in Fig. 2 is the equivalent source of HMIDC systems referred at LCC inverter ac bus i. When $\tilde{U}_i$ is taken as the reference vector and considering that $\tilde{Y}_{eqi}$ is almost inductive in the high voltage ac network, $E_{eqi}\angle\psi_{eqi}$ is then calculated as [13]

$$\begin{aligned}E_{eqi}\angle\psi_{eqi} &= \tilde{U}_i - \frac{\tilde{I}_{dci}}{\tilde{Y}_{eqi}} \approx U_i - \frac{(P_{di}-jQ_{di})^*/U_i}{-jY_{eqi}} \\ &= U_i - \frac{j(P_{di}+jQ_{di})/U_i}{Y_{eqi}} = U_i + \frac{Q_{di}}{U_i Y_{eqi}} - j\frac{P_{di}}{U_i Y_{eqi}}.\end{aligned} \tag{2}$$

In (2), the asterisk denotes the conjugate electrical quantity.

With the development of (2), it is known that TOV_i is actually equal to E_{eqi} when considering the system quasi-steady-state analytical model and thus can be calculated as

$$\begin{aligned}\mathrm{TOV}_i = E_{eqi} &= \sqrt{\left(U_i + \frac{Q_{di}}{U_i Y_{eqi}}\right)^2 + \left(\frac{P_{di}}{U_i Y_{eqi}}\right)^2} \\ &= \sqrt{U_i^2 + \left(\frac{Q_{di}}{U_i Y_{eqi}}\right)^2 + \frac{2Q_{di}}{Y_{eqi}} + \left(\frac{P_{di}}{U_i Y_{eqi}}\right)^2} \\ &= \sqrt{U_i^2 + \frac{P_{di}^2+Q_{di}^2}{U_i^2 Y_{eqi}^2} + \frac{2Q_{di}}{Y_{eqi}}}.\end{aligned} \tag{3}$$

It is worth mentioning that $\mathrm{HMIESCR}_i$ has been proposed to accurately depict the strength of HMIDC systems referred at LCC inverter ac bus i [13]. The mathematical expression of $\mathrm{HMIESCR}_i$ referring to Fig. 2 is given as

$$\mathrm{HMIESCR}_i = \frac{U_i^2 Y_{eqi}}{P_{di}}. \tag{4}$$

From which it is derived that

$$Y_{eqi} = \frac{\mathrm{HMIESCR}_i \cdot P_{di}}{U_i^2}. \tag{5}$$

Substituting (5) into (3) finally gives the mathematical expression of TOV_i as the analytical function of $\mathrm{HMIESCR}_i$ as

$$\begin{aligned}\mathrm{TOV}_i &= \sqrt{U_i^2 + \frac{P_{di}^2+Q_{di}^2}{U_i^2 Y_{eqi}^2} + \frac{2Q_{di}}{Y_{eqi}}} \\ &= \sqrt{U_i^2 + \frac{P_{di}^2+Q_{di}^2}{U_i^2 P_{di}^2\cdot\mathrm{HMIESCR}_i^2/U_i^4} + \frac{2Q_{di}}{P_{di}\cdot\mathrm{HMIESCR}_i/U_i^2}} \\ &= U_i\sqrt{1+\frac{2Q_{di}}{P_{di}}\cdot\frac{1}{\mathrm{HMIESCR}_i} + \frac{P_{di}^2+Q_{di}^2}{P_{di}^2}\cdot\frac{1}{\mathrm{HMIESCR}_i^2}}.\end{aligned} \tag{6}$$

C. On the Generalization

Since the TOV issue at LCC inverter ac buses due to the blocking of the LCC inverters is generally more serious than at VSC buses when VSC inverters are blocked, the primary focus in this letter has been put on LCC inverters in HMIDC systems. However, the theoretical analysis and derived equations in this section are still suitable for the TOV assessment at VSC buses if the blocking of the VSC inverters is further considered. This assertion can also be inferred from the related theoretical developments in the previous discussions, since there is no change on the final TOV mathematical expression in (6) even when the concerned LCC inverter is replaced by VSC. In other words, the derived (6) is actually generalized for the arbitrary case no matter when VSC or LCC inverters are concerned in the TOV analysis. Note also that in the analytical assessment of the TOV, the electrical quantities of P_d, Q_d, and HMIESCR should be provided for VSC or LCC inverters as can be clearly seen in the generalized (6).

III. Analytically Assessing the Effect of the HMIESCR on the TOV

A. Introduction of the Hybrid Tri-Infeed HVdc Test System

The hybrid tri-infeed HVdc test system (i.e., $n = 3$ in Fig. 1) is used for the analytical assessment here. In the test system, LCC inverters 1 and 2 feed power to ac buses 1 and 2, respectively, with the combination of the constant dc current and extinction angle control modes adopted. Also, VSC inverter 3 terminates at ac bus 3 with the combination of the constant active power and ac voltage control modes utilized. Moreover, the system parameters and operation variables for both LCC inverters are selected to be the same as in the CIGRE HVdc Benchmark Model [14], [15]. Meanwhile, $z_3 \angle \theta_3 = 0.5 \angle 74.96°$p.u., $z_{12} \angle \theta_{12} = z_{13} \angle \theta_{13} = z_{23} \angle \theta_{23} = 1.5 \angle 80.54°$p.u., $X_{T3} = 0.15$ p.u., $\tau_3 = 1.0$ p.u., $P_{d3} = 0.6$ p.u., $Q_{d3} = -0.2$ p.u. Note that when these values are changed subsequently, they are illustrated in the related explanations.

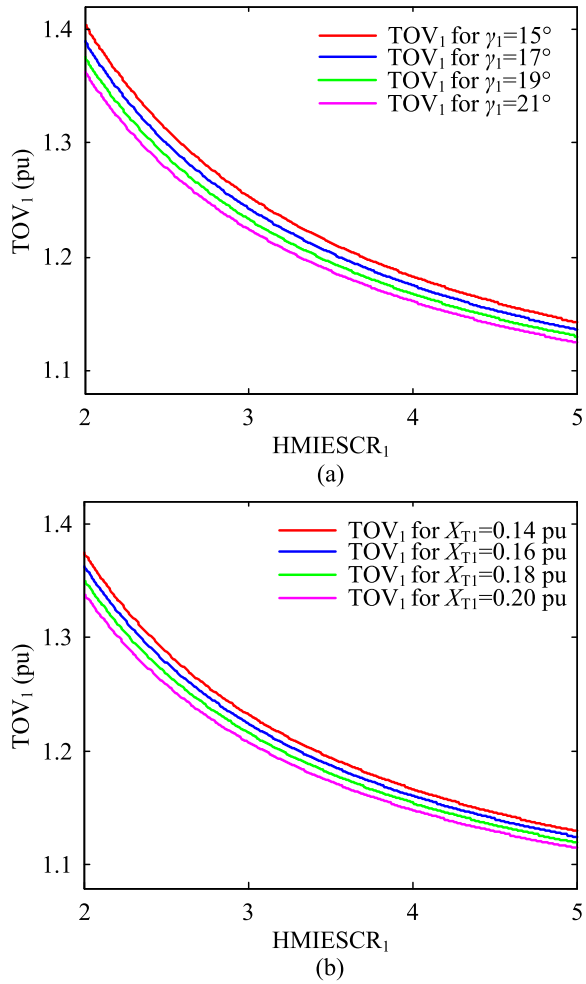

Fig. 3. Variation characteristics of TOV_1 versus $HMIESCR_1$ in the test system. (a) For each selected γ_1. (b) For each selected X_{T1}.

B. Analytically Assessing the Effect

The derived expression (6) is further used for analytically assessing the effect of the HMIESCR on the TOV versus various system parameters and operation variables in the test system based on the MATLAB program. For such purpose, consider TOV_1 at LCC inverter ac bus 1 for the blocking of LCC inverter 1. When the extinction angle of LCC inverter 1 (γ_1) is varied in the typical range from 15° to 21°, the variation characteristics of TOV_1 versus $HMIESCR_1$ are calculated using (6) and shown in Fig. 3(a). These characteristics are also given in Fig. 3(b) for the converter transformer leakage reactance (X_{T1}) changing in the typical range from 0.14 to 0.20 p.u. As can be first seen in Fig. 3(a) and (b), TOV_1 monotonically decreases along with the increasing $HMIESCR_1$ for each selected γ_1 or X_{T1}. This is understandable as a larger $HMIESCR_1$ means the stronger voltage support capability of the receiving end ac network to LCC inverter 1 at the concerned ac bus 1. Thus, a decreased TOV_1 is expected. Second, it is observed that the TOV_1-$HMIESCR_1$ curve is higher for a larger γ_1 or X_{T1}. This is because a larger γ_1 or X_{T1} indicates a higher Q_{d1} and hence greater TOV_1 under the certain $HMIESCR_1$ as inferred in (6). From the above discussions, it is clearly concluded that the HMIESCR has an inverse effect on the TOV in the test system.

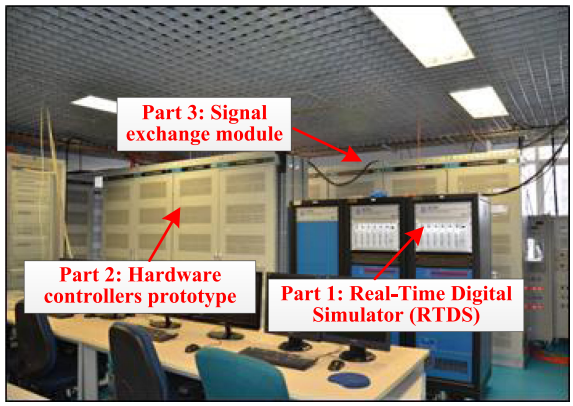

Fig. 4. Hardware-in-the-loop platform for the experimental results.

IV. Experimental Results

A. Description of the Hardware-in-the-Loop Platform

The hardware-in-the-loop platform for the experimental results of the test system in Section III-A is presented in Fig. 4, which comprises three separate parts. Part 1 represents the extensively used real-time digital simulator (RTDS) where the ac/dc main circuits such as dc lines, converters, transformers, reactive power compensators, and ac network are modeled. Moreover, Part 2 is the hardware prototype of the dc controllers for the control mode combination described previously. Meanwhile, the signal exchange module between Parts 1 and 2 is realized in Part 3 by using the analog-in and analog-out cards. More precisely, these signals include the dc current, extinction angle of LCC inverters 1 and 2, active power and ac bus voltage of VSC inverter 3.

B. Experimental Validation

Consider TOV_1 at LCC inverter ac bus 1 in the test system when LCC inverter 1 is blocked at $t = 1.2$ s in the hardware-in-the-loop platform in Fig. 4. Then for the variation of $HMIESCR_1$ in the pre-set range of interest from 2 to 5 with the steps of 1, TOV_1 for each selected γ_1 or X_{T1} is analytically calculated by (6) and shown in Tables I and II, respectively. In fact, these calculated values can also be obtained by referring to Fig. 3(a) and (b). For comparisons, the experimental TOV_1 is also observed accordingly for every $HMIESCR_1$. It is clearly seen in Tables I and II that the maximum errors between the calculated and experimental TOV_1 are 5.4% and 5.5%, respectively (marked by the bold font). These errors are deemed to be small enough for guiding the planning and operation of the practical HMIDC systems. In other words, the derived (6) and also analytical approach in Sections II and III are effectively validated by the experimental results of the test system.

TABLE I
EXPERIMENTAL RESULTS ON TOV_1 VERSUS $HMIESCR_1$ IN THE TEST SYSTEM FOR EACH SELECTED γ_1

$HMIESCR_1$		2	3	4	5
TOV_1 for γ_1=15°	Cal.	1.363	1.225	1.161	1.125
	Exp.	1.293	1.174	1.124	1.073
	Err.	**5.4 %**	4.3 %	3.3 %	4.8 %
TOV_1 for γ_1=17°	Cal.	1.376	1.234	1.168	1.130
	Exp.	1.324	1.189	1.117	1.075
	Err.	3.9 %	3.8 %	4.6 %	5.1 %
TOV_1 for γ_1=19°	Cal.	1.390	1.243	1.175	1.136
	Exp.	1.321	1.186	1.133	1.093
	Err.	5.2 %	4.8 %	3.7 %	3.9 %
TOV_1 for γ_1=21°	Cal.	1.405	1.254	1.183	1.143
	Exp.	1.348	1.198	1.136	1.090
	Err.	4.2 %	4.7 %	4.1 %	4.9 %

Cal.: Calculated. Exp.: Experimental. Err.: Error. Err. = |Cal. - Exp.|/Exp.

TABLE II
EXPERIMENTAL RESULTS ON TOV1 VERSUS HMIESCR1 IN THE TEST SYSTEM FOR EACH SELECTED XT_1

$HMIESCR_1$		2	3	4	5
TOV_1 for X_{T1}=0.14 pu	Cal.	1.339	1.208	1.149	1.115
	Exp.	1.284	1.149	1.091	1.070
	Err.	4.3 %	5.1 %	5.3 %	4.2 %
TOV_1 for X_{T1}=0.16 pu	Cal.	1.351	1.217	1.155	1.120
	Exp.	1.309	1.162	1.095	1.068
	Err.	3.2 %	4.7 %	**5.5 %**	4.9 %
TOV_1 for X_{T1}=0.18 pu	Cal.	1.363	1.225	1.161	1.125
	Exp.	1.302	1.182	1.118	1.082
	Err.	4.7 %	3.6 %	3.8 %	4.0 %
TOV_1 for X_{T1}=0.20 pu	Cal.	1.374	1.233	1.167	1.130
	Exp.	1.314	1.182	1.109	1.079
	Err.	4.6 %	4.3 %	5.2 %	4.7 %

Cal.: Calculated. Exp.: Experimental. Err.: Error. Err. = |Cal. - Exp.|/Exp.

C. Comparison With the Simulated Approach in Earlier Works

Although the research efforts have been made to evaluate the impact of the AISCR on the TOV in HMIDC systems [10], [11], this evaluation scheme is always achieved by the simulated approach. It is time-consuming because onerous electromagnetic transient simulations are required. For example, with simulations running on an Intel i7 processor, 1.80 GHz, 32.0 GB RAM personal laptop, it typically takes about 4 min to get the simulated TOV_1 for each selected γ_1 or X_{T1} under certain $HMIESCR_1$ in Tables I and II for the test system. Therefore, 128 min (around 2 h) are totally required for the 32 cases under investigation in both tables by the simulated approach in earlier works [10], [11]. As a comparison, only 1.8 s are needed in total for all the analytical calculations in both tables using (6) by the proposed analytical approach in this letter. The above discussions hence illustrate that compared to the simulated approach, the analytical approach is more efficient as no time-consuming simulations are required at all. It is further worth mentioning that as the effect of $HMIESCR_1$ on TOV_1 in the test system is analytically assessed in a more direct manner using (6) rather than analyzed by simulations, more sufficiently theoretical perspectives are able to be provided by the analytical approach.

V. CONCLUSION

This letter first derived the mathematical expression of the TOV as the analytical function of the HMIESCR by using the quasi-steady-state model of HMIDC systems with the interinverter interactions quantified by the MVIF. Second, the derived expression was used for analytically assessing the effect of the HMIESCR on the TOV. Compared with the simulated approach in earlier works, the proposed analytical approach could offer more sufficiently theoretical perspectives and was also more efficient because no time-consuming simulations were required at all. Finally, the analytical approach was validated by the experimental results of a hybrid tri-infeed HVdc test system based on the hardware-in-the-loop platform.

REFERENCES

[1] Y. Xue, X. Zhang, and C. Yang, "Series capacitor compensated ac filterless flexible LCC HVDC with enhanced power transfer under unbalanced faults," *IEEE Trans. Power Syst.*, vol. 34, no. 4, pp. 3069–3080, Jul. 2019.

[2] W. Xiang, S. Yang, G. P. Adam, H. Zhang, W. Zuo, and J. Wen, "DC fault protection algorithms of MMC-HVDC grids: Fault analysis, methodologies, experimental validations, and future trends," *IEEE Trans. Power Electron.*, vol. 36, no. 10, pp. 11245–11264, Oct. 2021.

[3] F. Zhang, H. Xin, D. Wu, Z. Wang, and D. Gan, "Assessing strength of multi-infeed LCC-HVDC systems using generalized short-circuit ratio," *IEEE Trans. Power Syst.*, vol. 34, no. 1, pp. 467–480, Jan. 2019.

[4] B. Zhou *et al.*, "Principle and application of asynchronous operation of China Southern Power Grid," *IEEE J. Emerg. Sel. Topics Power Electron.*, vol. 6, no. 3, pp. 1032–1040, Sep. 2018.

[5] B. Cheng, Z. Xu, and W. Xu, "Optimal dc-segmentation for multi-infeed HVDC systems based on stability performance," *IEEE Trans. Power Syst.*, vol. 31, no. 3, pp. 2445–2454, May 2016.

[6] B. Davies *et al.*, *Systems With Multiple DC Infeed*, CIGRE Working Group B4.41, 364, Dec. 2008.

[7] *IEEE Guide for Planning DC Links Terminating at AC Locations Having Low Short-Circuit Capacities*, IEEE Standard 1204-1997, Jun. 1997.

[8] E. Rahimi, "Voltage interactions and commutation failure phenomena in multi-infeed HVDC systems," Ph.D. dissertation, Dept. Elect. Comput. Eng., Winnipeg, MB, Canada, 2011.

[9] X. Chen, A. M. Gole, and M. Han, "Analysis of mixed inverter/rectifier multi-infeed HVDC systems," *IEEE Trans. Power Del.*, vol. 27, no. 3, pp. 1565–1573, Jul. 2012.

[10] C. Guo, Y. Zhang, A. M. Gole, and C. Zhao, "Analysis of dual-infeed HVDC with LCC-HVDC and VSC-HVDC," *IEEE Trans. Power Del.*, vol. 27, no. 3, pp. 1529–1537, Jul. 2012.

[11] Y. Zhang and A. M. Gole, "Quantifying the contribution of dynamic reactive power compensators on system strength at LCC-HVdc converter terminals," *IEEE Trans. Power Del.*, to be published, doi: 10.1109/TPWRD.2021.3063153.

[12] H. Xiao and Y. Li, "Multi-infeed voltage interaction factor: A unified measure of inter-inverter interactions in hybrid multi-infeed HVDC systems," *IEEE Trans. Power Del.*, vol. 35, no. 4, pp. 2040–2048, Aug. 2020.

[13] H. Xiao, Y. Zhang, X. Duan, and Y. Li, "Evaluating strength of hybrid multi-infeed HVDC systems for planning studies using hybrid multi-infeed interactive effective short-circuit ratio," *IEEE Trans. Power Del.*, vol. 36, no. 4, pp. 2129–2144, Aug. 2021.

[14] M. Szechtman, T. Wess, and C. V. Thio, "A benchmark model for HVDC system studies," in *Proc. Int. Conf. AC DC Power Transmiss.*, London, U.K., 1991, pp. 374–378.

[15] S. Mirsaeidi, D. Tzelepis, J. He, X. Dong, D. M. Said, and C. Booth, "A controllable thyristor-based commutation failure inhibitor for LCC-HVDC transmission systems," *IEEE Trans. Power Electron.*, vol. 36, no. 4, pp. 3781–3792, Apr. 2021.